Frontiers of Physics
https://doi.org/10.1007/s11467-019-0921-4
Front. Phys.
14(5), 52602 (2019)

RESEARCH ARTICLE

Entanglement and excited-state quantum phase transition in an extended Dicke model

Gui-Lei Zhu, Xin-You Lü†, Shang-Wu Bin, Cai You, Ying Wu

School of Physics, Huazhong University of Science and Technology, Wuhan 430074, China
Corresponding author. E-mail: †xinyoulu@hust.edu.cn
Received May 22, 2019; accepted August 8, 2019

We investigate the properties of entanglement and excited-state quantum phase transition (ESQPT) in a hybrid atom-optomechanical system in which an optomechanical quadratic interaction is introduced into a normal Dicke model. Interestingly, by preparing the ancillary mode in a coherent state, both the quantum entanglement and ESQPT can be realized in a relative weak-coupling condition. Moreover, the entanglement is immune to the A^2 term, and a reversed trend of the entropy is obtained when the A^2 term is included. Density of states (DoS) and Peres lattice are used to investigate ESQPTs. Compared to a normal Dicke model, the DoS enlarges $\exp(2r_\alpha)$ times if the ancillary mode is prepared in a coherent state. This work is an extension of the ground-state quantum phase transition, which may inspire further exploration of the quantum criticality in many-body systems.

Keywords phase transition, Dicke model

1 Introduction

Quantum phase transition (QPT) plays an important role in studying the nuclear, solid-state and many-body systems [1–7]. Briefly, QPT associating with the energy level crossing and symmetry breaking at critical point, describes an abrupt change in the ground state on account of quantum fluctuations. Different from thermal phase transitions, the QPTs occur at the absolute zero or near to zero temperature in which $\hbar\omega > k_BT$ was satisfied. Entanglement plays a key role in quantum computing, quantum cryptography and quantum teleportation [8]. It is found that the entanglement is closely bound up with QPT of the interacting many-body systems [9]. However, the QPT and the critical entanglement phenomenon are difficult to be realized in cavity QED systems, because of the restriction of so-called A^2 term [10–12].

Other than the ground-state QPT, latterly, another kind of phase transition: the excited-state quantum phase transition (ESQPT), have been studied in several many-body models [13–15]. The ESQPTs manifesting the simultaneous singularities of a certain critical energy E_c at a fixed control parameter, occur among states throughout the excitation spectra. The study of ESQPT is an extension of the quantum phase transition, which is closely connected with the existence of the barrier in the potential energy surface. In addition, recent years, the advances of the nano-fabricated technology, renew interests in the hybrid quantum model [16], e.g., cold atoms trapped in optical cavities [17–23], nitrogen-vacancy (NV) centers embedded in diamond nanobeam [24, 25]. Both these models can be described by an extended Dicke Hamiltonian [26]. One of the representative features of the Dicke Hamiltonian is the QPT from normal to superradiant behaviors, which is discovered by Hepp and Lieb [27]. Recent works show a close connection between QPTs, entanglement and onset of chaos in Dicke model [28–35]. Last several years, Perez-Fernández *et al.* [36, 37] pointed out the existence of an ESQPT of Dicke model. The previous works show that both entanglement and ESQPT can only occur in ultrastrong-coupling regimes, i,e, $\lambda \sim \omega$. Here we propose a hybrid quantum system combining the cavity QED and optomechanics, in which the entanglement and ESQPT can appear even in a relative weak-coupling condition, i.e., $\lambda \ll \omega$.

Here we focus on an atom-optomechanical system, in which a normal Dicke model couples to an ancillary optical mode with the form of optomechanical quadratic coupling [38–49], to investigate its entanglement and ESQPT. We find that both the entanglement and ESQPT show a photon-state-dependent property, i.e., they are controllable by preparing different states of the ancillary mode (vacuum state $|0\rangle_a$ or coherent state $|\alpha\rangle_a$). Specifically, if the ancillary mode is in a coherent state $|\alpha\rangle_a$, the system shows a lower threshold of atom-field coupling χ_c and the entanglement can be realized in a weak-coupling condition. Moreover, this entanglement is immune to the so-called A^2 term. More specifically, when the A^2 term is included, the entanglement exhibits a reversed trend to-

ward the increasing atom-field coupling.

Furthermore, here we employ the density of states and Peres lattices to investigate the ESQPT of the proposed system in coherent-states description. Interestingly, if the ancillary cavity mode is in $|\alpha\rangle_a$, the ESQPT can also occur in a weak-coupling condition, and the amplitude of density of states enhances exponentially compared with a normal Dicke model.

The structure of this paper is as follows. In Section 2 we describe the proposed model and give the Dicke-like Hamiltonian. We also analyze the photon-state and the A^2 term dependent entanglement of the hybrid Dicke Hamiltonian in this section. We employ the Hamiltonian in coherent-states description and obtain the classical Hamiltonian of our proposal in Section 3. In addition, Section 4 is devoted to describe the ESQPTs. Finally, we conclude our results in Section 5.

2 Model and Hamiltonian

As shown in Fig. 1, here we consider a normal Dicke model couples to an ancillary optomechanical cavity mode quadratically [49–51]. The system Hamiltonian is given by ($\hbar = 1$)

$$H_{\rm tot} = H_{\rm an} + H_{\rm dm} - g_0 a^\dagger a (b^\dagger + b)^2, \tag{1}$$

and we set

$$H_{\rm an} = \omega_c a^\dagger a, \tag{2}$$

$$H_{\rm dm} = \Omega J_z + \omega b^\dagger b + \frac{\lambda}{\sqrt{N}}(b^\dagger + b)J_x + \frac{\eta\lambda^2}{\Omega}(b^\dagger + b)^2, \tag{3}$$

where $a(a^\dagger)$ and $b(b^\dagger)$ are the annihilation (creation) operators of the ancillary cavity mode and the field mode of the Dicke Hamiltonian, respectively. The Hamiltonian $H_{\rm an}$ describes the ancillary cavity mode of the frequency ω_c, which quadratically couples to b with the coupling efficient g_0. It is clearly shown that the Dicke Hamiltonian $H_{\rm dm}$ has four parts: The first term refers to N two-level atoms which have the identical excited energy Ω. The second term represents the single-mode bosonic field with the frequency ω and the number operator $b^\dagger b$. The third term describes the atom-field interaction with the collective coupling strength λ, here the collective atomic pseudospin operators read $J_z = (1/2)\sum_{i=1}^N \sigma_z$, $J_\pm = \sum_{i=1}^N \sigma_\pm$, and $J_x = J_+ + J_-$, and they obey the SU_2 algebra. We point out that the so-called A^2 term is considered in last term. Generally speaking, based on the Thomas–Reiche–Kuhn sum rule [10], $\eta \geq 1$ corresponds to implementing Dicke model in a cavity QED system. $\eta = 0$ yields to the case of Hamiltonian $H_{\rm dm}$ reducing to a standard Dicke Hamiltonian. Here $\mathcal{N} = b^\dagger b + J_z + N/2$ counts the number of the total excitations of the system (excluding the ancillary mode a), and it is anticipated that the Hamiltonian

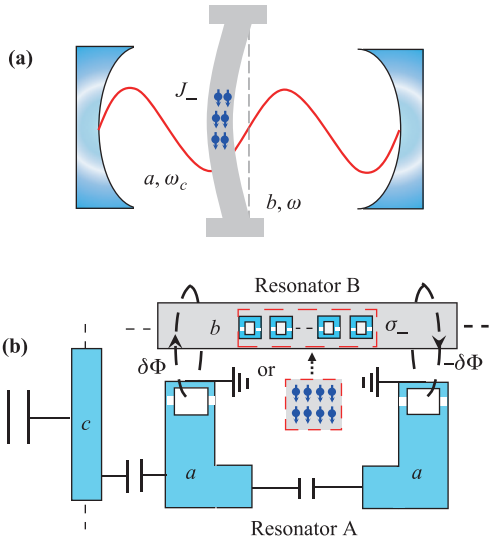

Fig. 1 The schematic diagram of the proposed system. **(a)** A schematic illustration of the proposed model in a quadratically-coupled optomechanical system. An ensemble of two-level atoms is embedded in a membrane (with bosonic mode b) with atom-field coupling strength λ, which describes the normal Dicke model. The single bosonic mode b interacts with an ancillary mode a with a quadratic coupling g_0, which can be realized by placing the membrane in the node of the cavity mode a. The mode a is prepared in a coherent state $|\alpha\rangle_a$. **(b)** A proposed implementation of the proposed system in a superconducting circuit with the ability of simulating a quadratic optomechanical coupling [45].

$H_{\rm tot}$ conserves parity operator $\Pi = {\rm e}^{{\rm i}\pi\mathcal{N}}$. Then the Hilbert space of $H_{\rm tot}$ can be separated into two noninteracting parts, due to the parity conservation as $[H_{\rm tot}, \Pi] = 0$.

In the following, we consider the ancillary mode a to be prepared in a vacuum state $|0\rangle_a$ or a coherent state $|\alpha\rangle_a$; then the photon-number operator $a^\dagger a$ could be replaced by an algebraic number 0 or $|\alpha|^2$. Even though the coherent state is not the eigenstate of the number operator $a^\dagger a$, and the fluctuation increases with the coherent state amplitude. However, the relative fluctuation (the ratio of fluctuation to the mean photon number) is $\sim 1/|\alpha|$. In other words, a larger coherent state amplitude α would result in a less relative fluctuation. Based on existing experimental implementation, cavity photon number up to 10^{10} has been realized [52], which manifests the effect of fluctuations can be ignored safely. Here we consider $|\alpha|^2 = 10^4$ for numerical calculations, in principle, the restriction on the amplitude could be relaxed largely and the quadratic coupling g_0 can be much weaker. Therefore, we could approximately use $|\alpha|^2$ to take place of $a^\dagger a$ for coherent states. We note that if the ancillary mode is prepared in a vacuum state, then the system Hamiltonian can be reduced into a normal Dicke model. In view of the quadratic coupling term and the A^2 term, we apply a squeezing transformation, i.e., $b = b_\alpha \cosh r_\alpha + b_\alpha^\dagger \sinh r_\alpha$; then we can obtain a simplified system Hamiltonian,

$$H_\alpha = \Omega J_z + \omega_\alpha b_\alpha^\dagger b_\alpha + \frac{\lambda_\alpha}{\sqrt{N}}(b_\alpha^\dagger + b_\alpha)J_x + C_\alpha \tag{4}$$

with the squeezing parameter

$$r_\alpha = -\frac{1}{4}\ln\left(1 + \eta\chi^2 - \frac{4|\alpha|^2 g_0}{\omega}\right), \tag{5}$$

and the rescaled coupling strength $\chi = 2\lambda/\sqrt{\Omega\omega}$ [53]. Here we obtained the effective frequency of the field mode $\omega_\alpha = \exp(-2r_\alpha)\omega$, and the effective atom-field coupling strength $\lambda_\alpha = \exp(r_\alpha)\lambda$, and $C_\alpha = |\alpha|^2\omega_c + [\exp(-2r_\alpha) - 1]\,(\omega/2)$ is a constant which merely results in the monolithic translation of energy level. Here we define the effective rescaled coupling $\chi_\alpha = \exp(2r_\alpha)\chi$. The Hamiltonian H_α shows a photon-state-dependent property. To be specific, if a is prepared in the vacuum state $|0\rangle_a$ ($\alpha = 0$), H_0 is a standard Dicke Hamiltonian. On this occasion, $\chi_c = 1$ for $\eta = 0$ and it is forbidden for $\eta \geq 1$ due to the no-go theorem. Nevertheless, if a is in a coherent state $|\alpha\rangle_a$, the rescaled critical coupling strength becomes $\chi_{\alpha c} = \exp(-2r_\alpha)$ and the restriction of the A^2 term is naturally broken up. Hereafter, for convenience, we only consider the case of $|0\rangle_a$ and $|\alpha\rangle_a$.

In the thermodynamic limit $N \to \infty$, The system Hamiltonian H_α yields a QPT of the second order, and the rescaled critical point reads $\chi_{\alpha c} = \exp(-2r_\alpha)$ in terms of the initial parameters. $\chi < \exp(-2r_\alpha)$ is related to the normal phase with a totally unexcited state ($\mathcal{N} = 0$ and $J_z = -j$). Otherwise when $\chi > \exp(-2r_\alpha)$, the system enters into the superradiant phase ($\mathcal{N} > 0$ and $-j < \langle J_z\rangle < j$). We note that the maximal value of j is $N/2$. When the A^2 term is considered, the occurrence of QPT requires $\chi > \sqrt{1 + \eta\chi^2 - 4|\alpha|^2 g_0/\omega}$, i.e.,

$$\chi^2 < \frac{1}{\eta - 1}\left(\frac{4|\alpha^2|g_0}{\omega} - 1\right). \tag{6}$$

In the left side of Eq. (6), $\chi^2 > 0$ is definitely satisfied. So in principle, this inequation can be satisfied only when

$$\frac{4|\alpha^2|g_0}{\omega} - 1 > 0. \tag{7}$$

In other words, only when $g_0 > \omega/(4|\alpha|^2)$, QPT would occur when considering A^2 term. This decides the parameter regime considered here.

In Fig. 2, the effective rescaled coupling strength χ_α versus the initial rescaled coupling χ and the quadratic optomechanical coupling g_0 is plotted. We could find that, for a given g_0, the χ_α increases with the increasing χ for taking no account of the A^2 term [see the black-dashed curve]. However, when the A^2 term is considered, the effective rescaled coupling χ_α shows an inverse trend toward χ, i.e., χ_α increases along with the decreasing χ (see the red-solid curve). The occurrence of this novel effect is due to a competition between the quadratic optomechanical interaction $g_0 a^\dagger a(b^\dagger + b)^2$ and the A^2 term $\eta\lambda^2/[\Omega(b^\dagger + b)^2]$

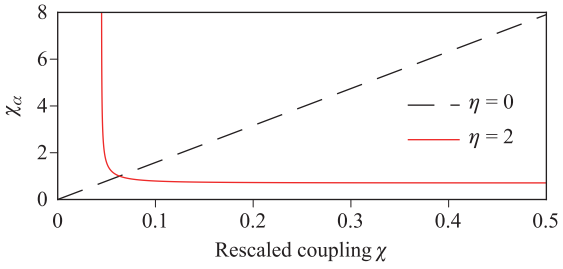

Fig. 2 The effective rescaled coupling strength χ_α with respect to χ. We consider the ancillary mode is in coherent state $|\alpha\rangle_a$. $\eta = 0, g_0 = 2.49 \times 10^{-5}\omega$ for black-dashed curve and $\eta = 2, g_0 = 2.51 \times 10^{-5}\omega$ for red-solid curve. Other parameters are $\omega = \Omega = 1$, and $|\alpha|^2 = 10^4$.

[49, 50]. When plotting Fig. 2, we considered two different parameter regimes. Specifically, $g_0 = 2.49 \times 10^{-5}$ for $\eta = 0$, in that if $\eta = 0$, the system would undergo a QPT when $g_0 < \omega/(4|\alpha|^2)$. Additionally, the case of $g_0 = 2.51 \times 10^{-5}$ when including the A^2 term, is restricted by Eq. (7).

We move forward to study the entanglement property for both including and ignoring the A^2 term. As a measure of the entanglement, we calculate the von Neumann entropy

$$S = -\mathrm{Tr}(\rho_b \log_2 \rho_b), \tag{8}$$

where ρ_b is the reduced density matrix of the field mode. Here we numerically calculate and plot the von Neumann entropy for finite N of our proposal, displayed in Fig. 3(a) for $\eta = 0$ (ignoring A^2 term) and in Fig. 3(b) for $\eta = 2$ (including A^2 term). Here the main panel shows ancillary mode a is in coherent state $|\alpha\rangle_a$, and the inserted panel shows the case of a in vacuum state $|0\rangle_a$. The exhibition of strong atom-field quantum entanglement shows many nontrivial properties; first, as is known to us that, for a normal Dicke model, the realization of quantum entanglement needs an ultra-strong coupling ($\chi \sim 1$). However, in our proposal, the strong entanglement can be realized in a relative weak-coupling condition, i.e., $\chi \ll 1$. Moreover, it breaks through the restriction of the A^2 term. In other words, the entanglement can occur for both considering and ignoring the A^2 term. Second, we find a reversed trend of the entropy occurs when the A^2 term being included [see Fig. 3(b)]. This fascinating effect is caused by the fact that when the A^2 term is considered, the effective rescaled coupling χ_α decreases along with an increasing rescaled coupling χ [see Fig. 2]. In other words, the system initially in the superradiant phase, and as the coupling χ increases, it would reach into the normal phase. Third, it was reported that in the thermodynamic limit (i.e., $N \to \infty$), the entropy would occur a divergence as approaching to the critical rescaled coupling $\chi_{\alpha c}$ [54]. In Fig. 3, this trend is obvious as the number of atoms increases.

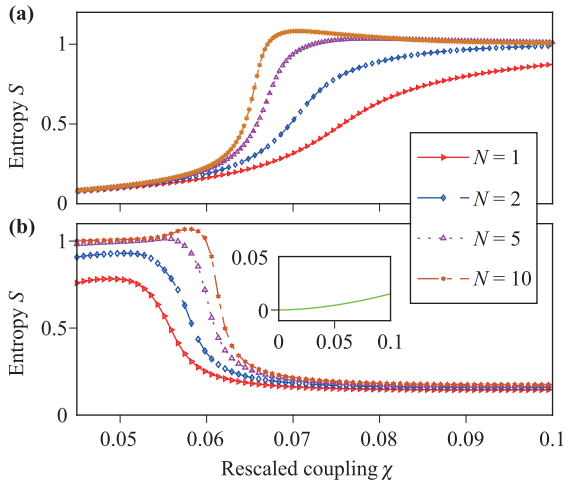

Fig. 3 The von Neumann entropy S corresponds to the rescaled coupling χ for different numbers of atoms N. Ancillary mode a is prepared in $|\alpha\rangle_a$ for the main panel and vacuum state $|0\rangle_a$ for the inserted panel. $\Omega = \omega = 1$, $|\alpha|^2 = 10^4$ for both, **(a)** $\eta = 0$ and $g_0 = 2.49 \times 10^{-5}\omega$ and **(b)** $\eta = 2$, $g_0 = 2.51 \times 10^{-5}\omega$ are considered, respectively.

3 Semiclassical Hamiltonians

In order to investigate the ESQPT of our proposal, we first present the Hamiltonian in a semiclassical description. The associated semiclassical Hamiltonian of H_α can be obtained in a coherent-state representation [55–57]. Different as before, here we employ Bloch and squeezed Glauber coherent states on the pseudospin sectors $J_i (i = x, z, \pm)$ and the bosonic mode b, respectively. These two states read

$$|z\rangle = \frac{1}{(1+|z|^2)^j} \mathrm{e}^{zJ_+} |j, -j\rangle, \tag{9}$$

$$\mathcal{S}(r_\alpha)|\beta\rangle = \mathrm{e}^{\frac{r_\alpha}{2}(b^{\dagger 2} - b^2)} \mathrm{e}^{-\frac{|\beta|^2}{2}} \mathrm{e}^{\beta b^\dagger} |0\rangle, \tag{10}$$

where z and β are complex numbers, and the overcomplete set $\{|z\rangle\}$ is normalized by $1 = \frac{2j+1}{\pi} \int |z\rangle\langle z| \frac{\mathrm{d}^2 z}{(1+|z|^2)}$. Here $\mathcal{S}(r_\alpha)$ is a squeezed operator applied on the coherent state $|\beta\rangle$. Physically, $\langle z, \mathcal{S}\beta|b|\mathcal{S}\beta, z\rangle = \langle z, \beta|b_\alpha|\beta, z\rangle$, here $b = \cosh(r_\alpha) b_\alpha + \sinh(r_\alpha) b_\alpha^\dagger$. That is to say, the expectation of b in a squeezed coherent state is equivalent to the squeezed mode b_α in a coherent state. To obtain the classical Hamiltonian, it is convenient to find the representation of the angular momentum and Weyl generators with respect to the tensorial product $|\beta, z\rangle = |\beta\rangle \otimes |z\rangle$,

$$H_{\mathrm{cl}}(\beta, z) = \langle \beta, z|H_\alpha|\beta, z\rangle = -j\Omega \left(\frac{1-|z|^2}{1+|z|^2}\right) + \omega_\alpha |\beta|^2 + \frac{\sqrt{2j}\lambda_\alpha}{(1+|z|^2)} (\beta^* + \beta)(z^* + z). \tag{11}$$

We move forward to represent H_{cl} using canonical variables. We take the harmonic oscillator realization for the field part and the stereographic projection for the angular momentum part, i.e.,

$$\beta = \frac{q + \mathrm{i}p}{\sqrt{2}}, \tag{12}$$

$$z = \mathrm{e}^{-\mathrm{i}\phi} \tan\frac{\theta}{2}, \tag{13}$$

where q, p are the real values, and $P = j_z = -j\cos\theta$ and $Q = \phi = \arctan(j_y/j_x)$ are the Bloch parameters. Here a classical vector $\boldsymbol{j} = (j_x, j_y, j_z)$ of the constant magnitude $|\boldsymbol{j}| = j$ has been constructed, and $\{P, Q\} = -1$ was satisfied, where θ and ϕ are the spherical angle variables. The classical Hamiltonian, in terms of the four canonical variables q, p, ϕ, j_z, reads

$$H_{\mathrm{cl}}(q, p, \phi, j_z) = \frac{\omega_\alpha}{2}(q^2 + p^2) + \Omega j_z + 2\lambda_\alpha \sqrt{j} \sqrt{1 - \left(\frac{j_z}{j}\right)^2}\, q\cos\phi. \tag{14}$$

From the Hamiltonian $H_{\mathrm{cl}}(q, p, \phi, j_z)$, we could derive the associated classical equations of motion,

$$\frac{\mathrm{d}q}{\mathrm{d}t} = \frac{\partial H_{\mathrm{cl}}}{\partial p} = \omega_\alpha\, p, \tag{15}$$

$$\frac{\mathrm{d}p}{\mathrm{d}t} = -\frac{\partial H_{\mathrm{cl}}}{\partial q} = -q\,\omega_\alpha - 2\lambda_\alpha \sqrt{j} \sqrt{1 - \frac{j_z^2}{j^2}} \cos\phi, \tag{16}$$

$$\frac{\mathrm{d}\phi}{\mathrm{d}t} = \frac{\partial H_{\mathrm{cl}}}{\partial j_z} = \Omega - \frac{2\lambda_\alpha j_z}{j^{3/2}\sqrt{1 - \frac{j_z^2}{j^2}}} q\cos\phi, \tag{17}$$

$$\frac{\mathrm{d}j_z}{\mathrm{d}t} = -\frac{\partial H_{\mathrm{cl}}}{\partial \phi} = 2\lambda_\alpha \sqrt{j} \sqrt{1 - \frac{j_z^2}{j^2}}\, q \sin\phi. \tag{18}$$

The rescaled ground-state energy has the form of

$$\epsilon_0(\chi) = \frac{E_0}{j\Omega} = \begin{cases} -1, & \text{for } \chi \le \chi_{\alpha c}, \\ -\frac{1}{2}(\chi_\alpha^2 + \chi_\alpha^{-2}), & \text{for } \chi > \chi_{\alpha c}. \end{cases} \tag{19}$$

To better visualize the property of the energy level, we fix the point of q, p by letting Eqs. (15, 16) equal to zero, then we construct energy surface in terms of the variables θ and ϕ,

$$\epsilon(\theta, \phi) = -\cos\theta - \frac{\chi_\alpha^2}{2}(1 - \cos^2\theta)\cos^2\phi. \tag{20}$$

Figure 4 plots the energy surface ϵ versus the variables θ and ϕ for different rescaled couplings considering the ancillary mode being prepared in two different states. The top row shows the results obtained in a normal Dicke model, i.e., A^2 term is ignored and the ancillary mode is prepared in the vacuum state $|0\rangle_a$. The middle shows the case of ancillary mode being in the coherent state $|\alpha\rangle_a$.

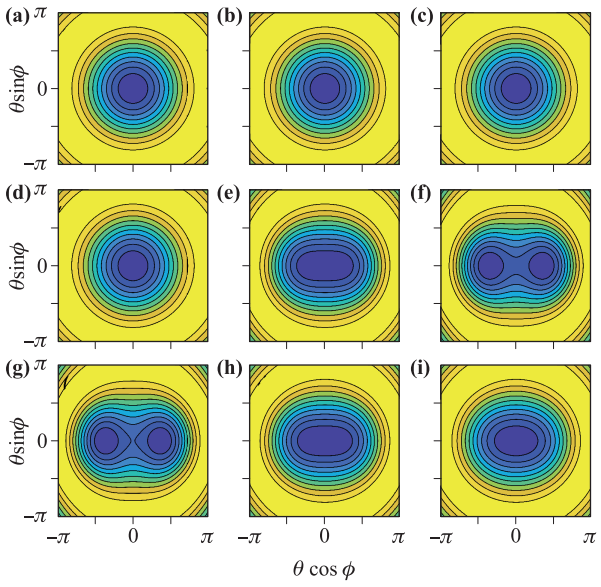

Fig. 4 Contourf of the energy surface ϵ versus θ and ϕ [see Eq. (20)]. In the top row, $\eta = 0$ and ancillary mode is prepared in vacuum state $|0\rangle_a$. From the left to right, the rescaled couplings are $0.01\omega, 0.064\omega, 0.096\omega$. The middle row shows the results considering $\eta = 0$, ancillary mode a in coherent state $|\alpha\rangle_a$. The rescaled couplings are same as the top row. The bottom shows $\eta = 2$, ancillary mode being in $|\alpha\rangle_a$. The parameters from left to right are $\chi = 0.05\omega, 0.064\omega, 0.096\omega$. respectively. Here $\chi_{\alpha c} = 2\lambda_\alpha/\sqrt{\Omega\omega_\alpha}$, $g_0 = 2.49 \times 10^{-5}\omega$ for $\eta = 0$ and $g_0 = 2.51 \times 10^{-5}\omega$ for $\eta = 2$ are considered.

We find that within the region considered, the energy surface, which is calculated from Eq. (20), essentially unchanged for $|0\rangle_a$. But it bifurcates into two separate parts as the effective atom-field coupling is increased through the critical point $\chi_{\alpha c}$ for $|\alpha\rangle_a$. Apparently, the minimum energy occurs at $\theta = 0$ (the blue-black areas indicated) for a coupling far below the critical point. Along with the increase of the coupling χ, the minimum energy degenerates at $\phi = 0, \pi$. The existence of the degeneration is associated with the spontaneous symmetry breaking. Physically, the $\mathcal{Z}_2$ symmetry reflected in the classical version as the invariance of the Hamiltonian $H_{\rm cl}$ is under the transformation of $(\phi, q) \to (\phi+\pi, -q)$ [58]. When the coupling strength χ crossing the critical point, the symmetry of the system is spontaneously broken up. In this case, the minimum energy levels become twofold degenerated. Comparison between Figs. 4(a)–(c) and Figs. 4(d)–(f), we find this bifurcation can appear at a much weaker-coupling condition ($\chi \ll 1$) when the mode a is in a coherent state.

Interestingly, it is shown in Figs. 4(g)–(i), when the A^2 term is considered, the bifurcation shows an inverse trend, i.e., the minimum energy would round up as the coupling χ increases. Physically, this is caused by the interplay between the quadratic optomechnical interaction and the A^2 term, which is analogous to the exhibition shown in Fig. 2. This result also shows an excellent agreement with the quantum entanglement [see Fig. 3(b)].

4 Excited-state quantum phase transition

It is well-established that the excited-state quantum phase transitions are marked by the presence of simultaneous singularities in the density of states (DoS) and order parameters [15, 59–63]. There are many methods to calculate the density of states in the classical approximation, here we adopt the method in Refs. [60, 61]. By considering $\Omega = \omega = 1$, then the density of the states in the proposed hybrid Dicke model reads

$$\frac{\omega_\alpha}{2j}\rho(\epsilon) = \begin{cases} \dfrac{1}{\pi}\displaystyle\int_{y_-}^{y_+} \arccos\sqrt{\frac{2(y-\epsilon)}{\chi_\alpha^2(1-y^2)}}\,{\rm d}y, & \epsilon_0 \le \epsilon < -1, \\ \dfrac{\epsilon+1}{2} + \dfrac{1}{\pi}\displaystyle\int_{\epsilon}^{y_+} \arccos\sqrt{\frac{2(y-\epsilon)}{\chi_\alpha^2(1-y^2)}}\,{\rm d}y, & |\epsilon| \le 1, \\ 1, & \epsilon > 1, \end{cases} \tag{21}$$

where

$$y_\pm = -\chi_\alpha^{-2} \pm \frac{\sqrt{2(\epsilon-\epsilon_0)}}{\chi_\alpha}. \tag{22}$$

We plot the DoS and its first derivative (inserted panel) versus ϵ for different values of χ in Fig. 5. As shown in Figs. 5(a, b), when $\chi \le \chi_{\alpha c}$, the singularity of DoS only appears at $\epsilon_c = 1$ and their first derivative occur the discontinuity at $\epsilon_c = 1$. For $\chi > \chi_{\alpha c}$, as is shown in Fig. 5(c), two singularities of the DoS occur at $\epsilon_c = \pm 1$, respectively. For ρ', a large cusp occurs at $\epsilon_c = -1$ and a discontinuity appears at $\epsilon_c = 1$. This fact verifies the appearance of ESQPT in our proposed system. Generally speaking, The critical energy $\epsilon_c = 1$ is related to the static ESQPT, which can occur for any values of the coupling. Moreover, the singularity at $\epsilon_c = -1$ is referred to the dynamic ESQPT, which can only appear in the superradiant phase [60, 61]. Interestingly, we find that the amplitudes of rescaled DoS considering the ancillary mode to be prepared in $|\alpha\rangle_a$, can be risen at $\exp(2r_\alpha)$ times in contrast to a normal Dicke model. Physically, this effect can be understood as follows: when the optomechanical interaction is considered and the ancillary mode to be prepared in a coherent state, the effective frequency of the single-bosonic

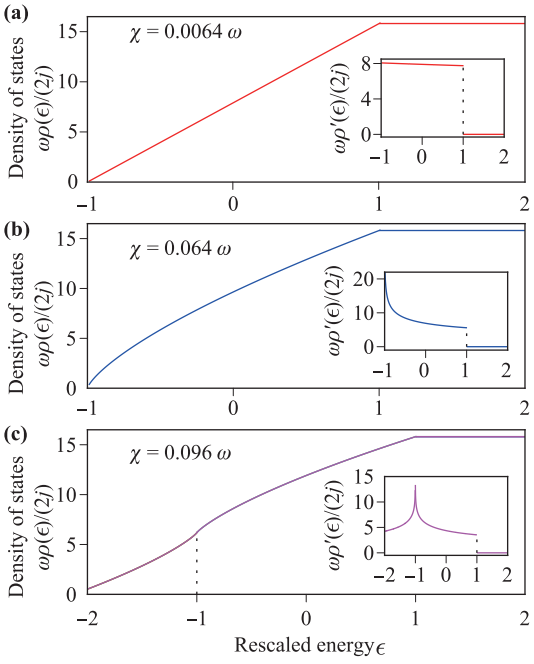

Fig. 5 The density of states $\rho(\epsilon)$, in units of $2j/\omega$, versus the the rescaled energy ϵ when mode a is in coherent state $|\alpha\rangle_a$. The inserted panels plot the first derivative of the density of states.

field is reduced largely, i.e., $\omega_\alpha \ll \omega$. In other words, the single-bosonic mode is effectively softened. Accordingly, the effective interaction between two-level ensemble and bosonic field is highly enhanced [47, 64]. It was reported that the factor $\mu = N\Omega/\omega \to \infty$ is crucial to characterize quantum phase transition [49]. In our model, the decreased ω_α renders μ enhanced effectively, which makes it easier to realize the quantum phase transition.

As one of indicators for the ESQPTs, the Peres lattice, proposed by Peres in 1984 [65], has been widely used to study the QPT and quantum chaos in many-body systems. Numerically, here the Peres lattices are constructed by calculating the expectation values of three different Peres operators, i.e., J_z, J_z^2 and J_x^2, in each eigenstate with eigenvalue ϵ. Here we consider $|0\rangle_a$ (upper row) and $|\alpha\rangle_a$ (bottom row), respectively. As shown in Fig. 6(a), when the ancillary mode is in $|0\rangle_a$, the distinguished cusp occurring at $\epsilon = 1$ is an indicative of singularity of the order parameter $\langle J_z\rangle/j$. Whereas for $|\alpha\rangle_a$, the Peres operator $\langle J_z\rangle$ occurs singularities in $\epsilon = \pm 1$ [see the black-dashed curve in Fig. 6(d)], which provides a compelling evidence on the discussion about Fig. 6(c). Furthermore, as is evidently shown in Figs. 6(e, f), when the ancillary mode is prepared in the coherent states, the expectation of Peres operators distributes in a wider energy region, and it present a transition from a regular pattern into the irregular one when crossing the $\epsilon_c = -1$, which clearly indicates the "trajectory" towards the onset of chaos from a classical integrable regime [28, 29, 36, 60, 61].

5 Conclusion

In conclusion, we have demonstrated the existence of the strong quantum entanglement and ESQPT in a relative weak-coupling condition. The quantum phase transition and entanglement of our proposal show a photon-state-dependent property. In other words, they lie on the different states of the ancillary cavity mode ($|0\rangle_a$ or $|\alpha\rangle_a$). We find the entanglement is immune to the so-called A^2 term

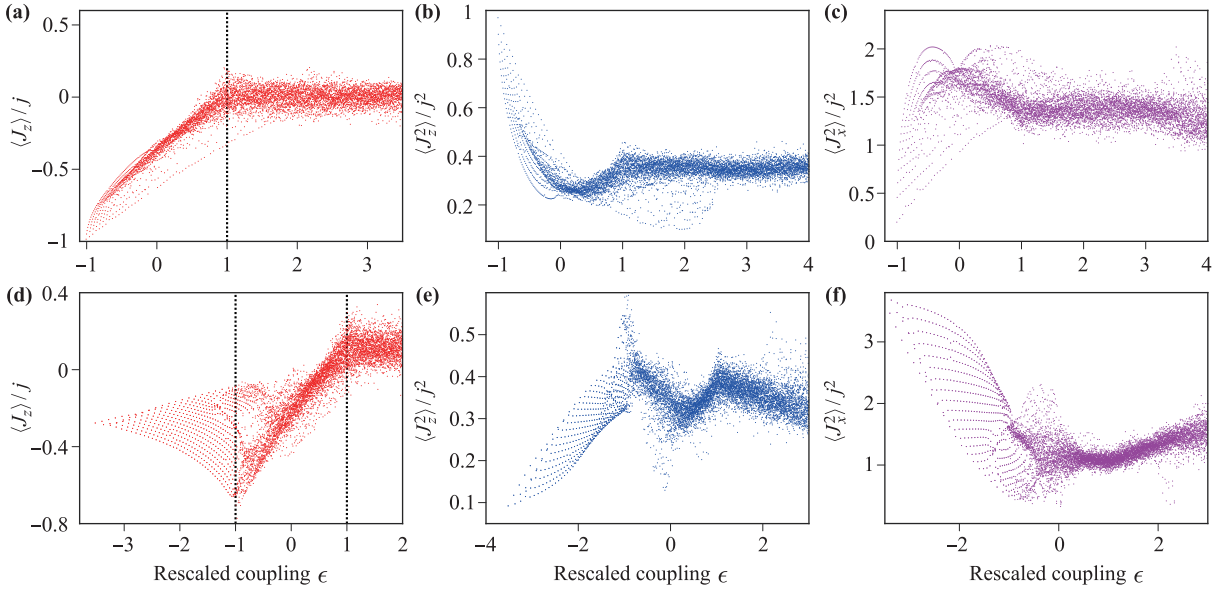

Fig. 6 Peres lattice of the proposed model using the Peres operators J_z (left panel), J_z^2 (middle panel) and J_x^2 (right panel) by considering a to be in $|0\rangle_a$ (upper row) and $|\alpha\rangle_a$ (bottom row). We use $j = 30$ and truncate $N_b^{\max} = 200$, $\Omega = \omega = 1$, $g_0 = 2.49 \times 10^{-5}\omega$, and $\chi = 0.99\omega$.

and a reversed trend of the entropy is obtained when the A^2 term is included. As anticipated, the ESQPT manifested by the DoS and Peres lattice, locates at a certain energy are observed in our proposal; and the analytical and numerical results show that the amplitude of DoS can be enlarged $\exp(2r_\alpha)$ times compared with the case of the ancillary mode being in a vacuum state.

The dissipation may affect the ground-state entanglement, but it can be approximately ignored in that here we considered a near closed system, not a dynamical one. To observe ground-state entanglement, a near zero temperature is needed, which can be realized by optical cooling [66]. Moreover, all the characteristic quantities of observing the ESQPT have scarce relation with dissipation or thermal noise. All these factors provide possibilities of experimental implementations. This work is fundamental in exploring the relation between quantum phase transition, entanglement and chaos of a hybrid quantum many-body systems.

Acknowledgements This work was supported by the National Key Research and Development Program of China under grant No. 2016YFA0301203, the National Natural Science Foundation of China (Grant Nos. 11822502, 11374116, 11574104, and 11375067), and the Fundamental Research Funds for the Central Universities under grant No. 2019kfyXMBZ054.

References

1. S. Sachdev, Quantum Phase Transitions, Cambridge: Cambridge University Press, 1999
2. S. L. Sondhi, S. M. Girvin, J. P. Carini, and D. Shahar, Continuous quantum phase transitions, *Rev. Mod. Phys.* 69(1), 315 (1997)
3. P. Cejnar, J. Jolie, and R. F. Casten, Quantum phase transitions in the shapes of atomic nuclei, *Rev. Mod. Phys.* 82(3), 2155 (2010)
4. R. F. Casten and E. A. McCutchan, Quantum phase transitions and structural evolution in nuclei, *J. Phys. G* 34(7), R285 (2007)
5. A. Osterloh, L. Amico, G. Falci, and R. Fazio, Scaling of entanglement close to a quantum phase transition, *Nature* 416(6881), 608 (2002)
6. J. Ma and X. Wang, Fisher information and spin squeezing in the Lipkin–Meshkov–Glick model, *Phys. Rev. A* 80(1), 012318 (2009)
7. T. L. Wang, L. N. Wu, W. Yang, G. R. Jin, N. Lambert, and F. Nori, Quantum Fisher information as a signature of the superradiant quantum phase transition, *New J. Phys.* 16(6), 063039 (2014)
8. R. Horodecki, P. Horodecki, M. Horodecki, and K. Horodecki, Quantum entanglement, *Rev. Mod. Phys.* 81(2), 865 (2009)
9. A. Osterloh, L. Amico, G. Falci, and R. Fazio, Scaling of entanglement close to a quantum phase transition, *Nature* 416(6881), 608 (2002)
10. P. Nataf and C. Ciuti, No-go theorem for superradiant quantum phase transitions in cavity QED and counterexample in circuit QED, *Nat. Commun.* 1(1), 72 (2010)
11. J. M. Knight, Y. Aharonov, and G. T. C. Hsieh, Are super-radiant phase transitions possible? *Phys. Rev. A* 17(4), 1454 (1978)
12. A. Vukics, T. Grießer, and P. Domokos, Elimination of the *A*-square problem from cavity QED, *Phys. Rev. Lett.* 112(7), 073601 (2014)
13. P. Cejnar and P. Stránský, Impact of quantum phase transitions on excited-level dynamics, *Phys. Rev. E* 78(3), 031130 (2008)
14. J. E. García-Ramos, P. Pérez-Fernández, and J. M. Arias, Excited-state quantum phase transitions in a two-fluid Lipkin model, *Phys. Rev. C* 95(5), 054326 (2017)
15. M. A. Caprio, P. Cejnar, and F. Iachello, Excited state quantum phase transitions in many-body systems, *Ann. Phys.* 323(5), 1106 (2008)
16. Z. L. Xiang, S. Ashhab, J. Q. You, and F. Nori, Hybrid quantum circuits: Superconducting circuits interacting with other quantum systems, *Rev. Mod. Phys.* 85(2), 623 (2013)
17. M. P. Baden, K. J. Arnold, A. L. Grimsmo, S. Parkins, and M. D. Barrett, Realization of the Dicke model using cavity-assisted Raman transitions, *Phys. Rev. Lett.* 113(2), 020408 (2014)
18. J. Klinder, H. Keler, M. Wolke, L. Mathey, and A. Hemmerich, Dynamical phase transition in the open Dicke model, *Proc. Natl. Acad. Sci. USA* 112(11), 3290 (2015)
19. J. M. Fink, R. Bianchetti, M. Baur, M. Göppl, L. Steffen, S. Filipp, P. J. Leek, A. Blais, and A. Wallraff, Dressed collective qubit states and the Tavis–Cummings model in circuit QED, *Phys. Rev. Lett.* 103(8), 083601 (2009)
20. D. Schneble, Y. Torii, M. Boyd, E. W. Streed, D. E. Pritchard, and W. Ketterle, The onset of matter-wave amplification in a superradiant Bose–Einstein Condensate, *Science* 300(5618), 475 (2003)
21. M. Scheibner, T. Schmidt, L. Worschech, A. Forchel, G. Bacher, T. Passow, and D. Hommel, Superradiance of quantum dots, *Nat. Phys.* 3(2), 106 (2007)
22. K. Baumann, C. Guerlin, F. Brennecke, and T. Esslinger, Dicke quantum phase transition with a superuid gas in an optical cavity, *Nature* 464(7293), 1301 (2010)
23. M. Greiner, O. Mandel, T. Esslinger, T. W. Haënsch, and I. Bloch, Collapse and revival of the matter wave field of a Bose–Einstein condensate, *Nature* 415, 39 (2002)
24. J. Teissier, A. Barfuss, P. Appel, E. Neu, and P. Maletinsky, Strain coupling of a nitrogen-vacancy center spin to a diamond mechanical oscillator, *Phys. Rev. Lett.* 113(2), 020503 (2014)
25. S. D. Bennett, N. Y. Yao, J. Otterbach, P. Zoller, P. Rabl, and M. D. Lukin, Phonon-induced spin–spin interactions in diamond nanostructures: Application to spin squeezing, *Phys. Rev. Lett.* 110(15), 156402 (2013)
26. R. H. Dicke, Coherence in spontaneous radiation processes, *Phys. Rev.* 93(1), 99 (1954)

27. K. Hepp and E. Lieb, On the superradiant phase transition for molecules in a quantized radiation field: The Dicke maser model, *Ann. Phys.* 76(2), 360 (1973)
28. C. Emary and T. Brandes, Quantum chaos triggered by precursors of a quantum phase transition: The Dicke model, *Phys. Rev. Lett.* 90(4), 044101 (2003)
29. C. Emary and T. Brandes, Chaos and the quantum phase transition in the Dicke model, *Phys. Rev. E* 67(6), 066203 (2003)
30. T. J. Osborne and M. A. Nielsen, Entanglement in a simple quantum phase transition, *Phys. Rev. A* 66(3), 032110 (2002)
31. N. Lambert, C. Emary, and T. Brandes, Entanglement and the phase transition in single-mode superradiance, *Phys. Rev. Lett.* 92(7), 073602 (2004)
32. G. Vidal, J. I. Latorre, E. Rico, and A. Kitaev, Entanglement in quantum critical phenomena, *Phys. Rev. Lett.* 90(22), 227902 (2003)
33. Q. H. Chen, Y. Y. Zhang, T. Liu, and K. L. Wang, Numerically exact solution to the finite-size Dicke model, *Phys. Rev. A* 78, 051801(R) (2008)
34. T. Liu, Y. Y. Zhang, Q. H. Chen, and K. L. Wang, Large-N scaling behavior of the ground-state energy, fidelity, and the order parameter in the Dicke model, *Phys. Rev. A* 80(2), 023810 (2009)
35. Y. Y. Zhang, X. Y. Chen, S. He, and Q. H. Chen, Analytical solutions and genuine multipartite entanglement of the three-qubit Dicke model, *Phys. Rev. A* 94(1), 012317 (2016)
36. P. Perez-Fernández, A. Relaño, J. M. Arias, P. Cejnar, J. Dukelsky, and J. E. García-Ramos, Excited-state phase transition and onset of chaos in quantum optical models, *Phys. Rev. E* 83(4), 046208 (2011)
37. P. Perez-Fernández and A. Relaño, from thermal to excited-state phase transition: The Dicke model, *Phys. Rev. E* 96(1), 012121 (2017)
38. M. Aspelmeyer, T. J. Kippenberg, and F. Marquardt, Cavity optomechanics, *Rev. Mod. Phys.* 86(4), 1391 (2014)
39. X. Y. Lü, Y. Wu, J. R. Johansson, H. Jing, J. Zhang, and F. Nori, Squeezed optomechanics with phase-matched amplification and dissipation, *Phys. Rev. Lett.* 114(9), 093602 (2015)
40. J. Q. Liao and F. Nori, Photon blockade in quadratically coupled optomechanical systems, *Phys. Rev. A* 88(2), 023853 (2013)
41. J. Q. Liao and F. Nori, Single-photon quadratic optomechanics, *Sci. Rep.* 4(1), 6302 (2014)
42. J. D. Thompson, B. M. Zwickl, A. M. Jayich, F. Marquardt, S. M. Girvin, and J. G. E. Harris, Strong dispersive coupling of a high-finesse cavity to a micromechanical membrane, *Nature* 452(7183), 72 (2008)
43. J. C. Sankey, C. Yang, B. M. Zwickl, A. M. Jayich, and J. G. E. Harris, Strong and tunable nonlinear optomechanical coupling in a low-loss system, *Nat. Phys.* 6(9), 707 (2010)
44. M. Bhattacharya, H. Uys, and P. Meystre, Optomechanical trapping and cooling of partially reflective mirrors, *Phys. Rev. A* 77(3), 033819 (2008)
45. E. J. Kim, J. R. Johansson, and F. Nori, Circuit analog of quadratic optomechanics, *Phys. Rev. A* 91(3), 033835 (2015)
46. H. K. Li, Y. C. Liu, X. Yi, C. L. Zou, X. X. Ren, and Y. F. Xiao, Proposal for a near-field optomechanical system with enhanced linear and quadratic coupling, *Phys. Rev. A* 85(5), 053832 (2012)
47. G. L. Zhu, X. Y. Lü, L. L. Wan, T. S. Yin, Q. Bin, and Y. Wu, Controllable nonlinearity in a dual-coupling optomechanical system under a weak-coupling regime, *Phys. Rev. A* 97(3), 033830 (2018)
48. C. S. Muñoz, A. Lara, J. Puebla, and F. Nori, Hybrid systems for the generation of nonclassical mechanical states via quadratic interactions, *Phys. Rev. Lett.* 121(12), 123604 (2018)
49. X. Y. Lü, L. L. Zheng, G. L. Zhu, and Y. Wu, Single-photon-triggered quantum phase transition, *Phys. Rev. Appl.* 9(6), 064006 (2018)
50. X. Y. Lü, G. L. Zhu, L. L. Zheng, and Y. Wu, Entanglement and quantum superposition induced by a single photon, *Phys. Rev. A* 97(3), 033807 (2018)
51. G. L. Zhu, X. Y. Lü, L. L. Zheng, Z. M. Zhan, F. Nori, and Y. Wu, Single-photon-triggered quantum chaos, *Phys. Rev. A* 100, 023825 (2019)
52. S. Gröblacher, K. Hammerer, M. R. Vanner, and M. Aspelmeyer, Observation of strong coupling between a micromechanical resonator and an optical cavity field, *Nature* 460(7256), 724 (2009)
53. M. Liu, S. Chesi, Z. J. Ying, X. Chen, H. G. Luo, and H. Q. Lin, Universal scaling and critical exponents of the anisotropic quantum Rabi model, *Phys. Rev. Lett.* 119(22), 220601 (2017)
54. A. Altland and T. Brandes, Quantum chaos and effective thermalization, *Phys. Rev. Lett.* 108(7), 073601 (2012)
55. F. T. Arecchi, E. Courtens, R. Gilmore, and H. Thomas, Atomic coherent states in quantum optics, *Phys. Rev. A* 6(6), 2211 (1972)
56. R. J. Glauber and F. Haake, Superradiant pulses and directed angular momentum states, *Phys. Rev. A* 13(1), 357 (1976)
57. M. A. M. de Aguiar, K. Furuya, C. H. Lewenkopf, and M. C. Nemes, Chaos in a spin-boson sytem: Classical analysis, *Ann. Phys.* 216(2), 291 (1992)
58. J. Chávez-Carlos, M. A. Bastarrachea-Magnani, S. Lerma-Hernández, and J. G. Hirsch, Classical chaos in atom-field systems, *Phys. Rev. E* 94(2), 022209 (2016)
59. P. Stránský, M. Macek, and P. Cejnar, Excited-state quantum phase transitions in systems with two degrees of freedom: Level density, level dynamics, thermal properties, *Ann. Phys.* 345, 73 (2014)
60. M. A. Bastarrachea-Magnani, S. Lerma-Hernández, and J. G. Hirsch, Comparative quantum and semiclassical analysis of atom-field systems (I): Density of states and excited-state quantum phase transitions, *Phys. Rev. A* 89(3), 032101 (2014)

61. M. A. Bastarrachea-Magnani, S. Lerma-Hernández, and J. G. Hirsch, Comparative quantum and semiclassical analysis of atom-field systems (II): Chaos and regularity, *Phys. Rev. A* 89(3), 032102 (2014)

62. P. Perez-Fernández, P. Cejnar, J. M. Arias, J. Dukelsky, J. E. García-Ramos, and A. Relaño, Quantum quench influenced by an excited-state phase transition, *Phys. Rev. A* 83(3), 033802 (2011)

63. T. Brandes, Excited-state quantum phase transitions in Dicke superradiance models, *Phys. Rev. E* 88(3), 032133 (2013)

64. X. Y. Lü, W. M. Zhang, A. Ashhab, Y. Wu, and F. Nori, Quantum-criticality-induced strong Kerr nonlinearities in optomechanical systems, *Sci. Rep.* 3(1), 2943 (2013)

65. A. Peres, New conserved quantities and test for regular spectra, *Phys. Rev. Lett.* 53(18), 1711 (1984)

66. D. Kleckner and D. Bouwmeester, Sub-kelvin optical cooling of a micromechanical resonator, *Nature* 444(7115), 75 (2006)